Hindawi
Wireless Communications and Mobile Computing
Volume 2018, Article ID 2835741, 11 pages
https://doi.org/10.1155/2018/2835741

Research Article

Performance Analysis of PN Code Acquisition with MIMO Scheme for an UWB TH/CDMA System

Yu Min Hwang,[1] **Eun Cheol Kim**,[2] **and Jin Young Kim**[1]

[1]*Department of Wireless Communications Engineering, Kwangwoon University, Seoul, Republic of Korea*
[2]*LG Electronics. Co. Ltd., Seoul, Republic of Korea*

Correspondence should be addressed to Jin Young Kim; jinyoung@kw.ac.kr

Received 27 June 2018; Accepted 9 October 2018; Published 18 October 2018

Academic Editor: Dajana Cassioli

This paper presents performance and its simulation results of pseudonoise (PN) code acquisition scheme with MIMO scheme for an ultra-wideband time-hopping/code-division-multiple-access (UWB TH/CDMA) system. The transmission channel is modelled as a frequency selective lognormal fading channel. In almost practical PN code acquisition system, the existence of more than two synchronous cells in the uncertainty region of the search process is possible due to multipath effect. Therefore, based on deriving the detection probability, false alarm rate, miss detection probability, and mean acquisition time, the acquisition performance is analyzed under the hypothesis of multiple synchronous states (cells) in the uncertainty region of the PN code. And the code acquisition performance is evaluated when the correlator outputs are noncoherently combined by using equal gain combining (EGC) scheme. In this procedure, the closed form for the conditional probability of decision variable is derived using the Gauss-Hermite quadrature formula. The performance comparison of the scheme mentioned above shows that the code acquisition performance with the diversity combining technique, especially when increasing the number of antenna, is more robust than that using no diversity. And code acquisition performance comparison also shows that if the detection threshold is set inappropriately, the performance might be degraded, even if an antenna diversity method is applied. It is also shown that Tx diversity can improve the acquisition performance but not as much as Rx diversity does. And Rx diversity can be applied to the acquisition system for additional diversity gain if the complexity of the receiver can be accepted.

1. Introduction

UWB (ultra-wideband) systems have been considered in several commercial and military communication applications due to several advantageous features such as low transmission power requirement, high data rate, robustness to severe multipath, low probability of intercept, and fine delay resolution property. One of the critical parts for successful development of the UWB systems is synchronization between transmitted and received signals because the UWB signal has the extremely narrow time frames and high sampling rates. In a typical approach, the encoded data symbols introduce a time dither on generated pulses leading to the so-called time hopping UWB (TH-UWB). Direct-sequence spread spectrum (DSSS) in the impulse radio version indicated as direct sequence UWB (DS-UWB) has been known to be an attractive solution to implement the impulse radio signals [1, 2].

In an UWB TH/CDMA (time-hopping/code-division-multiple-access) system, data demodulation is possible only after a receiver accurately synchronizes the locally generated pseudo noise (PN) code with the received one. The procedure of the PN code synchronization is usually divided into two steps: code acquisition (for coarse code alignment) and code tracking (for fine alignment) [3]. The PN code acquisition is the procedure to achieve synchronization between the received PN code and the locally generated PN code within one or half chip. After the PN code acquisition has been achieved, code tracking loop starts its operation. The PN code tracking is the procedure to make and keep the remaining phase difference to be a minimum value (typically, zero). Compared with PN code tracking, the PN code acquisition is usually known to be a more difficult task and has a great impact on the overall system performance [4]. In this paper,

we focus on PN code acquisition of the UWB signals in the UWB TH/CDMA systems.

Typical UWB systems use low signal power and very large signal bandwidth. Moreover, the UWB channel is a dense multipath channel without significant fading. Therefore, the energy of the signal is spread over several paths and the energy of each path is very low. This phenomenon has a bad influence on code acquisition of the UWB signals. The paths containing low power are difficult to acquire. Therefore, the acquisition system for the UWB signals should properly use the energy contained in the dense multipath. A practical way to acquire the energies of the several paths is to perform equal gain combining (EGC) [5].

In UWB systems, multiple access interference (MAI) may cause performance degradation so that the throughput of systems is reduced. There are several techniques to enhance the system performance. One of them is to use the selective maximal ratio combiners (or S-RAKE receivers). But as the number of RAKE fingers increases the performance enhancement is insignificant and the complexity of the receiver grows proportionally with the number of RAKE fingers. Other effective methods are diversity combining techniques using multiple antennas at a transmitter and a receiver, respectively, which can improve signal to noise ratio (SNR) [6, 7]. Receive antenna diversity (Rx diversity) schemes can improve the code acquisition performance higher than transmit antenna diversity (Tx diversity) schemes do. But in practical wireless mobile environments, Rx diversity schemes are not appropriate choice. The reason is that according as the number of antennas increases at the receiver, the receiver complexity also increases. So the size of handheld device is enlarged, the price of that is raised, and the power consumption of that increases. Therefore, Tx diversity schemes have received more and more attention to improve the acquisition performance and to reduce the receiver complexity in wireless communication systems [8].

In this paper, we analyze a PN code acquisition performance for the UWB TH/CDMA system using Tx and Rx diversity schemes which improve the signal quality at the receiver. The proposed diversity technique is that the transmitter sends the UWB signals from multiple transmitting antennas using time delays. In order to investigate the effect of multiple antennas at a receiver and to achieve additional improvement in the performance with the combination of Tx and Rx diversities, the conventional Rx diversity scheme is adopted. Before code acquisition is achieved, the receiver has no idea about any timing phase information on the received signals. And non-coherent combining schemes can be applied without timing phase information on the received signals. So in our analysis, noncoherent equal gain combining scheme is applied for collecting the energies available in the multipath components. In almost practical PN code acquisition systems, it is possible that there exist more than two synchronous cells in the uncertainty region of the search process due to multipath effects. So it is assumed that there are multiple synchronous cells in the uncertainty region of the PN code. In accordance with the number of Tx and Rx antennas, the system performance is analyzed over the frequency-selective lognormal fading channel. The closed form formula for the conditional probability density function (PDF) of decision variable is derived when the signal with Gaussian distribution goes through the lognormal fading channel. The performance is analyzed through deriving the formulas for detection probability, false alarm rate, miss detection probability, and mean acquisition time of the proposed system.

The remainder of this paper is organized as follows. Section 2 describes the signal and channel models. Then, the proposed system is described in Section 3. In Section 4, the proposed system performance is analyzed. In order to analyze the performance, the statistics of the decision variables associated with the EGC scheme and the expressions for the detection probability, false alarm rate, miss detection probability, and mean acquisition time are derived in the lognormal fading channel. The simulation results for the proposed system are presented in Section 5, and concluding remarks are given in Section 6.

2. Signal and Channel Models

2.1. Transmitter Signal. We consider an array of M identical transmitting antennas, sufficiently separated in space to eliminate correlation between antenna elements. For a UWB TH/CDMA system using an impulse radio, the transmitted signal of the u^{th} user from the m^{th} transmitter antenna can be expressed as

$$S^{u}_{tr,m}(t) = \sqrt{\frac{P}{M}} \sum_{j=-\infty}^{\infty} \sum_{k=0}^{N_f-1} W_{tr}\left[t - \left(jN_f + k\right)T_f - \Omega(u,k)\,T_c - \delta D_j - \tau^{u}_{m}\right], \tag{1}$$

where P is the transmitted power, W_{tr} is transmitted signal monocycle waveform, T_c is the chip duration, and δ is PPM (pulse position modulation) index chosen to optimize performance. Each antenna's transmit power is reduced to P/M in order that the total transmit power is identical regardless of the number of transmitter antennas. N_f and T_f are the number of time frames per symbol period and the frame length, respectively. $\Omega(u,k)$ denotes the random time hopping code matrix, in which u^{th} row represents the time hopping pattern of the u^{th} user. u^{th} row is made up of a random permutation of integers. The data in the j^{th} bit period is denoted by D_j, which is modeled as a wide-sense stationary random process composed of equally likely binary symbols $D_j \in \{0, 1\}$. And τ^{u}_{m} is the intentional time delay of the m^{th} antenna which is introduced before the transmission. It is assumed that $[\tau^{u}_{m}/T_c]$ is an integer.

2.2. Channel Model. We assume that the propagation channel is modeled by the UWB indoor channel model described in [3]. This model gives a statistical distribution for the path gains based on a UWB propagation experiment. Because of the frequency sensitivity of the UWB channel, the pulse shapes with different excess delays are path-dependent [9]. Also, it is assumed that the pulse shapes associated with all the propagation paths are identical. Then, the channel impulse

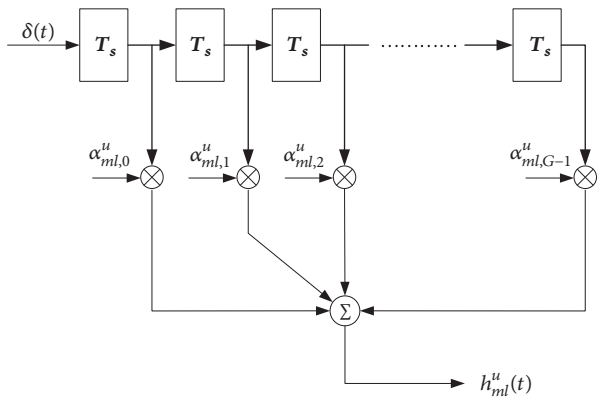

Figure 1: Tapped-delay-line model of the frequency selective fading channel.

response (CIR) can be modeled as a tapped-delay-line (TDL) structure, which is shown in Figure 1.

Assuming U active transmitters, the CIR of the signal transmitted from the m^{th} antenna of the u^{th} user ($u = 0, 1 \ldots, U-1$) and received by the l^{th} antenna can be expressed as

$$h^u_{ml}(t) = \sum_{g=0}^{G-1} \alpha^u_{ml,g} \delta\left(t - gT_s\right), \tag{2}$$

where G is the number of resolve multipath components, $\alpha^u_{ml,g}$ is the complex channel fading coefficient for the g^{th} path at excess delay $(g-1)T_s$, $\delta(t)$ is the Dirac delta function, and T_s is the minimum multipath resolvable interval, which depends on the bandwidth of the transmitted signal monocycle waveform $W_{tr}(t)$.

In this paper, it is suggested the CIR for the UWB signal in an indoor environment be modelled as a TDL structure with lognormal distributed coefficients [10, 11]. Though some other possible fading models, such as Rayleigh, Rice, Nakagami, and Suzuki (or mixed) distributions, can be applicable to the UWB indoor channel, the lognormal fading model is known to have passed goodness-of-fit tests based on the Kolmogorov-Smirnov procedure [12] and proved the supremacy of lognormal distribution in describing the amplitudes over different local areas as well as indoor areas with 90% confidence.

2.3. Receiver Signal. It is assumed that the combining scheme is non-coherent equal gain combining and the propagation time delay of the signal from the m^{th} antenna of the u^{th} transmitter to the l^{th} receiver antenna is $\tau^u_{ml,g}$, which is an independent random variable uniformly distributed in $[0, T_s)$. And we consider an array of L identical receiving antennas, sufficiently separated in space to eliminate correlation between antenna elements. The input signal to each receiver antenna is corrupted by additive white Gaussian noise (AWGN) with two-sided power spectral density of $N_0/2$. The received signal in the multiuser multipath environment at the l^{th} receiver antenna, $r_l(t)$, is given by

$$r_l(t) = \sum_{m=0}^{M-1} \sum_{u=0}^{U-1} \sum_{g=0}^{G-1} \alpha^u_{ml,g} S^u_{tr,m}\left(t - \tau_g\right) + n_l(t), \tag{3}$$

where τ_g is the total path delay of the g^{th} path which includes $\tau^u_{ml,g}$. The last term of the equation, $n_l(t)$, represents AWGN with zero mean and variance σ^2_{nl}. The minimum multipath resolvable interval, T_s, is not explicitly represented in (3); however it affects the distribution of $\tau^u_{ml,g}$. Since the distances between each pair of transmitter antenna and receiver antenna are approximately same all over m and l, it can be assumed that all the signals arrive at L receiver antennas simultaneously; in other words, the difference of the arrival timings of the signals between different receiver antennas is negligibly small. Therefore, the phase offset of the PN code is common for all over the M and L antennas. Since the fading characteristics of different pairs of transmitter and receiver antennas are assumed to be mutually independent, $\alpha^u_{ml,g}$ is an independently and identically distributed (i.i.d.) lognormal random variable with a PDF [2], when $\alpha^u_{ml,g}$ is greater than or equal to zero,

$$f_{\alpha^u_{ml,g}}(\omega) = \frac{1}{\omega\sqrt{2\pi\left(\sigma^u_{ml,g}\right)^2}} \exp\left(-\frac{\left(\ln\omega - \mu^u_{ml,g}\right)^2}{2\left(\sigma^u_{ml,g}\right)^2}\right), \tag{4}$$

where ω is a realization of $\alpha^u_{ml,g}$, $\mathrm{E}[\omega^2] = (\sigma^u_{ml,g})^2$ and $\mu^u_{ml,g}$ and $\sigma^u_{ml,g}$ are mean and standard deviation of $\ln\omega$, respectively.

3. System Description

In this paper, it is assumed that each transmitter has M antennas and the UWB signals are sent with different time delay, τ^u_m, to achieve Tx diversity. It's also assumed that there are L antennas at the receiver for additional diversity gain. In order to guarantee that the signals between each pair of transmitter and receiver antennas fade independently, each transmitter and receiver antenna are spatially separated from others by several wavelengths of the carrier. The block diagrams of the proposed transmitter and receiver for a UWB TH/CDMA system are illustrated in Figures 2 and 3. And it is assumed that the search step size is $T_c/2$. The threshold value T is determined by using the cell averaging-constant false alarm rate (CA-CFAR) algorithm [13].

The internal structure of the correlator in Figure 3 is described in Figure 4. The l^{th} correlator, $l = 0, 1, \ldots, L-1$, is a conventional active and dump correlating element. All correlators are associated with the same phase of the local despreading code. And the outputs of the L correlators are combined into one decision variable V which is given by a sum of correlator outputs $X_0, X_1, \ldots, X_{L-1}$. This combining scheme is EGC. Then, the decision variable V is compared to a threshold T to decide whether codes are aligned or not.

Then, the search and detection procedure can be explained as follows. The search mode employs the serial

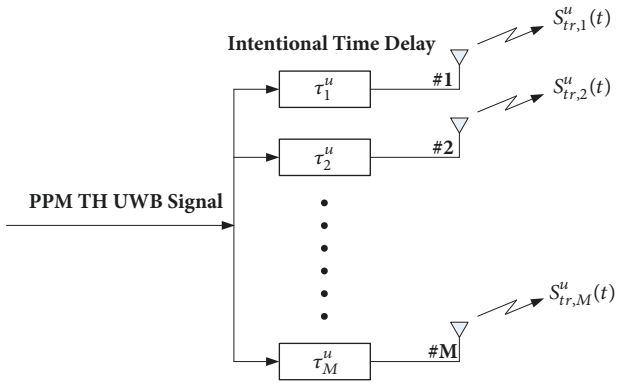

FIGURE 2: Transmitter model.

search strategy. Whenever the decision variable V exceeds the threshold T, the system decides that the corresponding delay of the locally generated PN sequence is the correct one and enters the verification mode. If V does not exceed T, the phase of a locally generated PN sequence is rejected. Then, another phase is chosen to update the decision variable and above operation is repeated.

4. Performance Analysis

The correlator output, X_l, $l = 0, 1, \ldots, L-1$, of Figure 3 can be expressed as

$$\begin{aligned} X_l &= \int_{jT_f}^{(j+1)T_f} r_l(t)\, S^u_{rec}(t)\, dt \\ &= \sum_{m=0}^{M-1} \sum_{u=0}^{U-1} \sum_{g=0}^{G-1} \alpha^u_{ml,g} \int_{jT_f}^{(j+1)T_f} S^u_{tr,m}\left(t-\tau_g\right) S^u_{rec} dt \\ &\quad + \int_{jT_f}^{(j+1)T_f} n_l(t)\, S^u_{rec} dt, \end{aligned} \tag{5}$$

where (5) is valid for any j and $S^u_{rec}(t)$ is the receiver template signal, which is denoted as

$$S^u_{rec}(t) = \sqrt{\frac{P}{M}} \sum_{m=0}^{M-1} \sum_{j=-\infty}^{\infty} \sum_{k=0}^{N_f-1} W_{rec}\left[t - \left(jN_f + k\right)T_f - \Omega(u,k)\,T_c - \delta D_j - \tau^u_m\right], \tag{6}$$

In this paper, it is assumed that there is no frequency error. And the channel is an indoor environment channel where the amplitude of signals is lognormally distributed.

The correlator output, X_l, of the UWB system approximately has Gaussian distribution with mean μ_{X_l} and variance $\sigma^2_{X_l}$. The random variable, X_l, is a sum of M independent and identically distributed random variables. And it has shown that regardless of statistical dependence, the expected value of a sum of random variables is equal to the sum of the expected values by the central limit theorem. It has also shown that the variance of a sum of random variables is equal to the sum of the individual variances if each random variable is independent [14–16]. So μ_{X_l} and $\sigma^2_{X_l}$ can be expressed as

$$\mu_{X_l} = \sum_{m=0}^{M-1} \mu_{S_m}, \tag{7}$$

$$\sigma^2_{X_l} = \sum_{m=0}^{M-1} \sigma^2_{S_m}, \tag{8}$$

where μ_{S_m} and σ_{S_m}, $m = 0, 1, \ldots, M-1$, are the mean and standard deviation of the transmitted signals $S^u_{tr,m}(t)$ for each t, respectively.

If an H_1 cell is being tested, the PDF of X_l can be expressed as

$$f_x\left(x \mid H_1, \mu_{X_l}\right) = \frac{1}{\sqrt{2\pi\sigma^2_{X_l}}} \exp\left(-\frac{\left(x-\mu_{X_l}\right)^2}{2\sigma^2_{X_l}}\right). \tag{9}$$

And if an H_0 cell is being tested, the PDF of X_l can be expressed as

$$f_x\left(x \mid H_0\right) = \frac{1}{\sqrt{2\pi\sigma^2_{X_l}}} \exp\left(-\frac{x^2}{2\sigma^2_{X_l}}\right). \tag{10}$$

The equal gain combiner output, V, of the UWB receiver also has Gaussian distribution with mean μ_V and variance σ^2_V.

$$\mu_V = \sum_{l=0}^{L-1} \mu_{X_l}, \tag{11}$$

$$\sigma^2_V = \sum_{l=0}^{L-1} \sigma^2_{X_l}, \tag{12}$$

Therefore, the conditional PDF of V associated with an H_1 cell can be expressed as

$$f_V\left(v \mid H_1, \mu_V\right) = \frac{1}{\sqrt{2\pi\sigma^2_V}} \exp\left(-\frac{\left(x-\mu_V\right)^2}{2\sigma^2_V}\right). \tag{13}$$

For a UWB TH/CDMA system using Tx diversity of M antenna elements, the transmitted signals from M transmitter antennas are summed and received at each receiver antenna. And by using Rx diversity of L antenna elements and EGC, L branches are equally weighted and summed. Therefore, the PDF of a sum of independent lognormal random variables (RVs) is necessary to derive the PDF of the decision variable, V, when an H_1 cell or an H_0 cell is tested. Though there

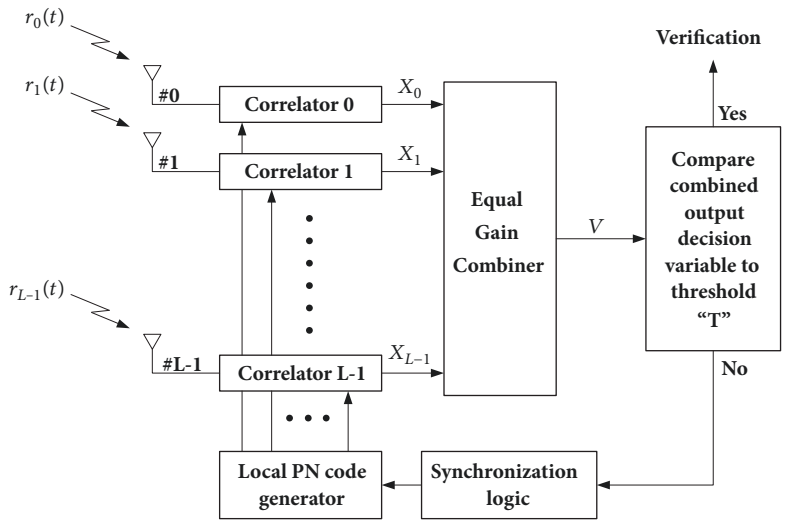

Figure 3: Receiver model.

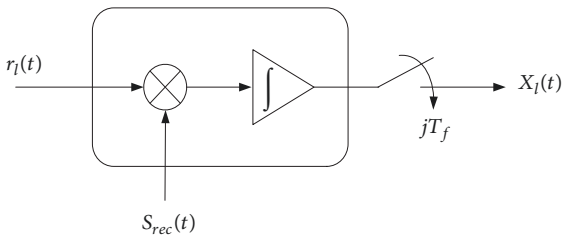

Figure 4: Structure of correlator in Figure 3.

does not exist a closed form expression for it, such a form can be approximated by another lognormal RV. One of the approximation methods is the Wilkinson's method [17].

Let $\mu_Y = \exp(Y)$, where Y, $Y \sim N(\mu_Y, \sigma_Y^2)$, is a normal RV. In Wilkinson's method, the two parameters μ_Y and σ_Y are obtained by matching the first two moments of μ_V with the first two moments of $\sum_{l=0}^{L-1} \mu_{X_l}$. These two parameters are given as

$$\mu_Y = \ln\left(\frac{E_{L1}^2}{\sqrt{E_{L2}}}\right), \tag{14}$$

$$\sigma_Y = \sqrt{\ln\left(\frac{E_{L2}}{E_{L1}^2}\right)}, \tag{15}$$

where E_{L1} and E_{L2} are, respectively, given by

$$E_{L1} = \sum_{l=0}^{L-1} \exp\left\{2\left(\mu_{X_l} + \sigma_{X_l}^2\right)\right\}. \tag{16}$$

$$\begin{aligned} E_{L2} = {} & \sum_{l=0}^{L-1} \exp\left\{4\left(\mu_{X_l} + \sigma_{X_l}^2\right)\right\} \\ & + 2\sum_{b=1}^{L-2}\sum_{c=b+1}^{L-1} \exp\left\{4\left(\mu_{X_b} + \mu_{X_c} + \sigma_{X_b}^2 + \sigma_{X_c}^2\right)\right\}. \end{aligned} \tag{17}$$

Then, when μ_V is greater than or equal to zero, the approximated PDF of μ_V is obtained as

$$f\left(\mu_V\right) = \frac{1}{\mu_V\sqrt{2\pi\sigma_Y^2}} \exp\left(-\frac{\left(\ln\mu_V - \mu_Y\right)^2}{2\sigma_Y^2}\right). \tag{18}$$

The conditioning in (13) may be removed by using

$$f_V\left(v \mid H_1\right) = \int_{-\infty}^{\infty} f_V\left(v \mid H_1, \mu_V\right) f\left(\mu_V\right) d\mu_V. \tag{19}$$

Substituting (13) and (18) into (19), we have

$$\begin{aligned} f_V\left(v \mid H_1\right) = {} & \frac{1}{2\pi\sigma_V\sigma_Y} \int_0^{\infty} \frac{1}{\mu_V} \exp\left(-\frac{\left(v - \mu_V\right)^2}{2\sigma_V^2}\right) \\ & \cdot \exp\left(-\frac{\left(\ln\mu_V - \mu_Y\right)^2}{2\sigma_Y^2}\right) d\mu_V. \end{aligned} \tag{20}$$

Letting $\ln\mu_V = r$, then

$$\begin{aligned} f_V\left(v \mid H_1\right) = {} & \frac{1}{2\pi\sigma_V\sigma_Y} \int_0^{\infty} \exp\left(-\frac{\left(v - \exp\left(r\right)\right)^2}{2\sigma_V^2}\right) \\ & \cdot \exp\left(-\frac{\left(r - \mu_Y\right)^2}{2\sigma_Y^2}\right) dr. \end{aligned} \tag{21}$$

And letting $(r - \mu_Y)/\sqrt{2}\sigma_Y = z$, the resulting PDF after some algebra can be expressed as

$$\begin{aligned} f_V\left(v \mid H_1\right) = {} & \frac{1}{\sqrt{2}\pi\sigma_V} \int_{-\infty}^{\infty} \exp\left(-z^2\right) \\ & \cdot \exp\left(-\frac{\left(v - \exp\left(\sqrt{2}\sigma_Y z + \mu_Y\right)\right)^2}{2\sigma_V^2}\right) dz. \end{aligned} \tag{22}$$

The above integral expression is efficiently and accurately evaluated using the Gauss-Hermite quadrature formula [17], which can be expressed as

$$\int_{-\infty}^{\infty} f(x) \exp\left(-x^2\right) dx \approx \sum_{i=1}^{I} h_{x_i} f\left(x_i\right), \tag{23}$$

where $f(x)$ is an arbitrary real function, I is the quadrature order (determining approximation accuracy), x_i, $i = 1, 2, \ldots, I$, are the zeroes of the I^{th} order Hermite polynomial, and h_{x_i} are the Gauss-Hermite quadrature weight factors in [18, p. 890].

Then, by treating

$$f(z) = \exp\left(-\frac{\left(v - \exp\left(\sqrt{2}\sigma_Y z + \mu_Y\right)\right)^2}{2\sigma_V^2}\right), \tag{24}$$

we can derive the following closed form for the PDF of V when an H_1 sample is being tested. It can be expressed as

$$\begin{aligned} f_V(v \mid H_1) &= \frac{1}{\sqrt{2}\pi\sigma_V} \int_{-\infty}^{\infty} f(z) \exp\left(-z^2\right) dz \\ &\approx \sum_{i=1}^{I} \frac{h_{z_i}}{\sqrt{2}\pi\sigma_V} \exp\left(-\frac{\left(v - \exp\left(\sqrt{2}\sigma_Y z_i + \mu_Y\right)\right)^2}{2\sigma_V^2}\right). \end{aligned} \tag{25}$$

Furthermore, the PDF of V with an H_0 cell can be expressed as

$$f_V(v \mid H_0) = \frac{1}{\sqrt{2\pi\sigma_V^2}} \exp\left(-\frac{v^2}{2\sigma_V^2}\right), \tag{26}$$

The detection probability for a given value of the decision threshold is defined as the probability of the event that the output decision variable corresponding to an H_1 cell exceeds the decision threshold, which can be obtained by

$$P_D = \int_T^{\infty} f_V(v \mid H_1) dv, \tag{27}$$

where P_D represents the detection probability of an H_1 cell, T represents the decision threshold, and $f_V(v \mid H_1)$ is given by (25). Upon substituting (25) into the above equation, it can be derived that

$$\begin{aligned} P_D &\approx \int_T^{\infty} \sum_{i=1}^{I} \frac{h_{z_i}}{\sqrt{2}\pi\sigma_V} \\ &\quad \cdot \exp\left(-\frac{\left(v - \exp\left(\sqrt{2}\sigma_Y z_i + \mu_Y\right)\right)^2}{2\sigma_V^2}\right) dv \\ &= \frac{1}{\sqrt{2}\pi\sigma_V} \sum_{i=1}^{I} h_{z_i} \\ &\quad \cdot \int_T^{\infty} \exp\left(-\frac{\left(v - \exp\left(\sqrt{2}\sigma_Y z_i + \mu_Y\right)\right)^2}{2\sigma_V^2}\right) dv. \end{aligned} \tag{28}$$

Letting $\exp(\sqrt{2}\sigma_Y z_i + \mu_Y) = K(z_i)$, then

$$\begin{aligned} P_D &\approx \frac{1}{\sqrt{\pi}} \sum_{i=1}^{I} \frac{h_{z_i}}{\sqrt{2\pi\sigma_V^2}} \int_T^{\infty} \exp\left(-\frac{\left(v - K\left(z_i\right)\right)^2}{2\sigma_V^2}\right) dv \\ &= \frac{1}{\sqrt{\pi}} \sum_{i=1}^{I} h_{z_i} Q\left(\frac{T - K\left(z_i\right)}{\sigma_V}\right). \end{aligned} \tag{29}$$

The threshold coefficient T is determined from the false alarm probability associated with a H_0 cell. The false alarm probability is defined as the probability of the event that the output decision variable corresponding to a H_0 cell exceeds the decision threshold, which can be expressed as

$$P_{FA} = \int_T^{\infty} f_V(v \mid H_0) dv, \tag{30}$$

where P_{FA} is the false alarm probability and $f_V(v \mid H_0)$ is given by (26). Upon substituting (26) into (30) and performing the required integrations, the false alarm probability can be obtained by

$$P_{FA} = \int_T^{\infty} \frac{1}{\sqrt{2\pi\sigma_V^2}} \exp\left(-\frac{v^2}{2\sigma_V^2}\right) dv = Q\left(\frac{T}{\sigma_V}\right), \tag{31}$$

Not only Holmes and Chen [19] but also Polydoros and Weber [19] have derived the equation for computing the mean acquisition time (MAT) for a serial search code acquisition system in both exact and asymptotic forms under the single H_1-cell and double H_1-cell hypotheses in the uncertainty region. And Lie-Liang and Lajos [20] have given a generalized asymptotic equation for the MAT under the multiple H_1-cell hypothesis.

The equivalent circular state diagram for a serial search code acquisition system with multiple H_1-cell hypothesis is drawn in Figure 5. P_D is replaced by $1 - \beta_i$ for notation convenience and β_i represents the miss probabilities of the i^{th} detection, leading to $\beta_i = 1 - P_D$. Nodes represent states, branches between two nodes indicate state transitions, z represents the unit-delay operator, and the power of z represents the time delay. The branch gains in a transform domain are derived accordingly, which are

$$H_D(z) = \sum_{j=1}^{\lambda} (1 - \beta_i) z \prod_{i=1}^{j-1} \beta_i z, \tag{32}$$

$$\prod_{i=1}^{0} \beta_i z = 1, \tag{33}$$

$$H_0(z) = (1 - \alpha) z + \alpha z^{k+1}, \tag{34}$$

$$H_M(z) = P_M(\lambda) z^{\lambda}, \tag{35}$$

where α represents the false alarm probability associated with an H_0 cell, λ is the number of H_1 cells in the uncertainty region to be searched, and $H_D(z)$ and $H_M(z)$ include all paths leading to successful detection or miss detection, respectively.

Table 1: Parameter settings for simulation.

Parameters	Values
PN sequence of length	1,023
q, which determines the length of the uncertainty region	2,046
search step size	$T_c/2$
α, false alarm rate	0.001
J, penalty time constant	1,000
L, receiver antennas	$\{1, 2, 4\}$
M, transmit antennas	$\{1, 2, 4, 8\}$
U, the number of users	10
$J\tau_D$, penalty time	$1,000\tau_D$
τ_D, the integral dwell time	$64T_c$
τ_m^u, intentional time delay	$4T_c$

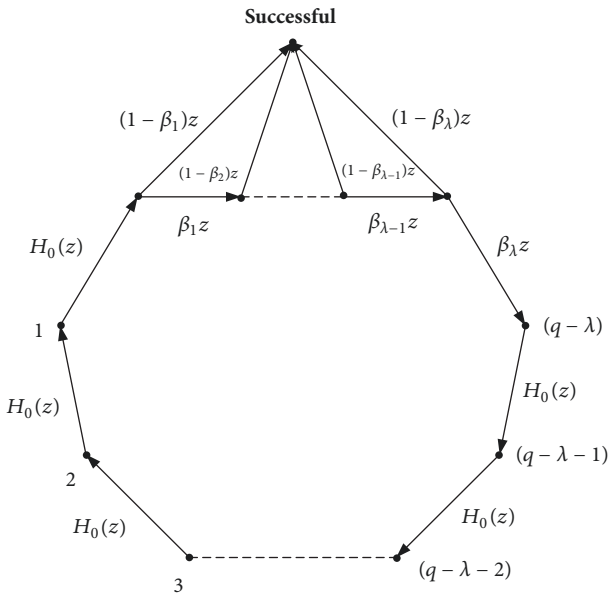

Figure 5: Equivalent circular state diagram for a serial search code acquisition system with multiple timing hypotheses.

$P_M(\lambda)$ represents the overall miss detection probability of a search over the full uncertainty region, which can be expressed as [20–22]

$$P_M(\lambda) = \prod_{i=1}^{\lambda} (1 - P_D). \tag{36}$$

The transfer function, $H(z)$, assuming equal prior probability of each state can be expressed as

$$H(z) = \frac{H_D(z)}{(q-\lambda)\left[1 - H_M(z)\, H_0^{q-\lambda}(z)\right]} \sum_{i=0}^{j-1} H_0^i(z), \tag{37}$$

where q is the number of total states in the uncertainty region of the PN sequence. In the approximation, it is assumed that $q \gg 1$.

The mean acquisition time of the proposed system, $E(T_{acq})$, is derived using the state diagram in Figure 5. From the transfer function (37) and branch gains in (32)-(35), the generalized expression for the asymptotic mean acquisition time of the proposed serial search acquisition system with single or multiple adjacent H_1 cells is given by

$$\overline{T}_{acq} = \frac{\left[1 + P_M(\lambda)\right]\left(1 + JP_{FA}\right)}{2\left[1 - P_M(\lambda)\right]} \left(q\tau_D\right), \tag{38}$$

where $J\tau_D$ represent the 'penalty time' associated with determining if there is a false alarm and re-entering the search mode.

5. Simulation Results

In this section, the code acquisition performance of a UWB TH/CDMA system using Tx and Rx diversities is evaluated. To verify the performance of the proposed system, its detection probability, miss detection probability, and mean acquisition time are tested using various system parameters in frequency-selective lognormal fading channel. The performance of Tx diversity is also compared with that of Rx diversity. The system performance is analyzed in terms of the number of transmit and receive antennas. As an application for the serial search is considered, we use a PN sequence of length 1,023. Therefore, q, which determines the length of the uncertainty region, is 2,046 since the search step size is assumed to be half of the chip duration. For convenience, the normalized mean acquisition time, which is derived from (38) divided by T_c, is considered. All results are evaluated from (27), (30), (36), and (38). For the analysis, the false alarm rate is set at 0.001 and the penalty time constant, J, is set at 1,000. The other parameters for simulations are tabulated in Table 1.

In Figure 6, the detection probability versus the SNR per chip performance for the proposed system is shown in accordance with the number of transmit antenna. As expected, because of the SNR enhancement with the diversity combining technique, the detection probability increases as the number of antennas increases. But the degree of improvement in detection probability gradually decreases with the number of antennas.

In Figure 7, the miss detection probability versus the SNR per chip performance is depicted in accordance with

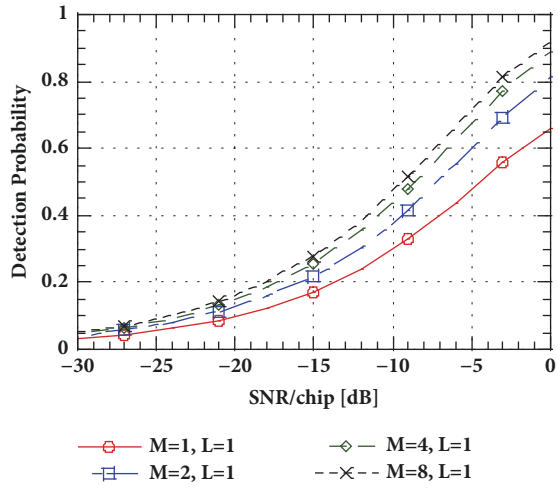

FIGURE 6: Detection probability versus SNR per chip performance for the proposed system with various transmit antennas (L=1, M=1, 2, 4, 8).

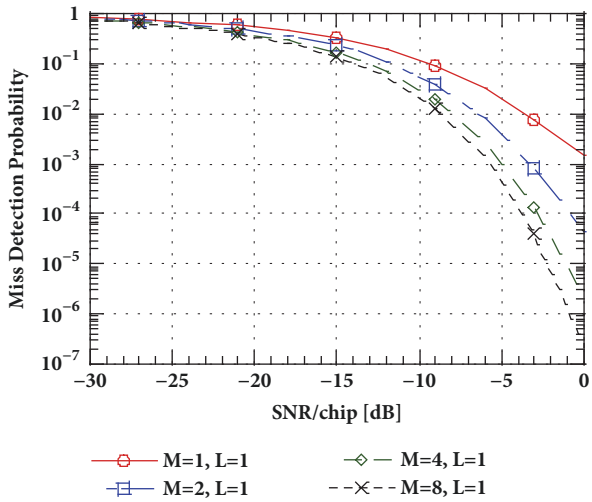

FIGURE 7: Miss detection probability versus SNR per chip performance for the proposed system with various transmit antennas (L=1, M=1, 2, 4, 8).

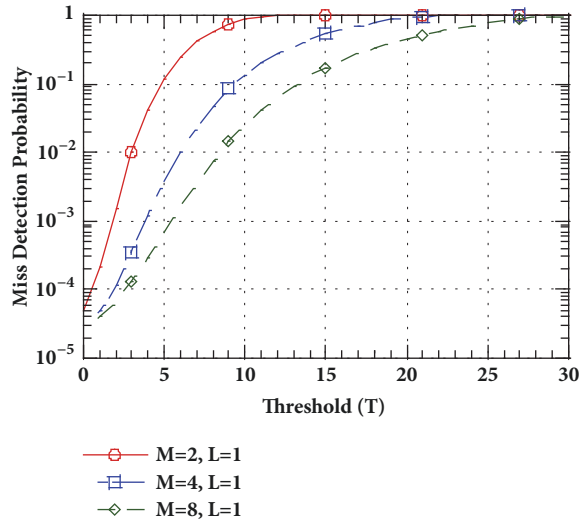

FIGURE 8: Miss detection probability versus threshold, T, performance for the proposed system with various transmit antennas when SNR/chip=-4dB (L=1, M=2, 4, 8).

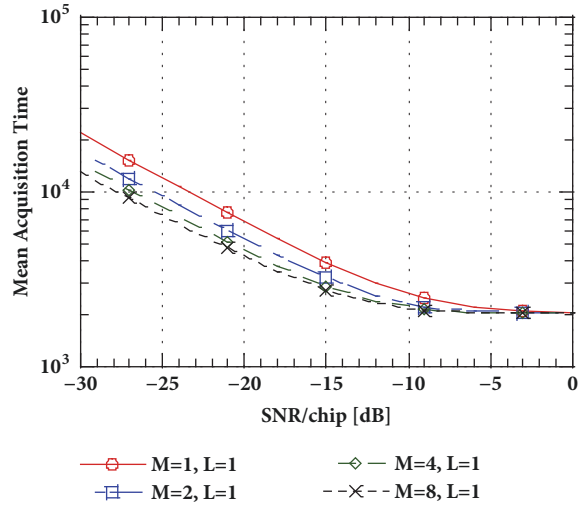

FIGURE 9: Mean acquisition time versus SNR/chip per chip performance for the serial search acquisition of the proposed system with various transmit antennas (L=1, M=1, 2, 4, 8).

the number of transmit antenna. We can see that the miss detection probability decreases; however, the rate of decrease increases as the number of antenna increases. This phenomenon is observed since the SNR increases with Tx diversity scheme.

In Figure 8, we evaluate and compare the overall miss detection probability versus the threshold, T, performance with various transmit antennas for the proposed system. SNR/chip is set at -4dB. As expected, the overall miss detection probability of the proposed system using Tx diversity increases with the threshold T. And the necessary threshold value to maintain the required miss detection probability increases as the number of antennas increases.

In Figure 9, the mean acquisition time versus the SNR per chip performance with the number of transmit antenna is shown. As the number of antennas increases from one to two, two to four, or four to eight, the mean acquisition time decreases. When the SNR/chip is over -6dB, the mean acquisition time performance becomes almost identical, regardless of the number of antennas. The reason of this is that the miss detection probability is under 10^{-1} when the SNR/chip is over -6dB in Figure 7. Therefore, the miss detection probability term in (37) hardly affects the mean acquisition time.

In Figure 10, the mean acquisition time performance of the proposed system is presented against the threshold, T. There is an optimal choice of the threshold, T, which leads to the minimum mean acquisition time. If the value of the threshold is set inappropriately, the mean acquisition time will significantly increase as the number of transmit antenna decreases. We can also find that the mean acquisition time

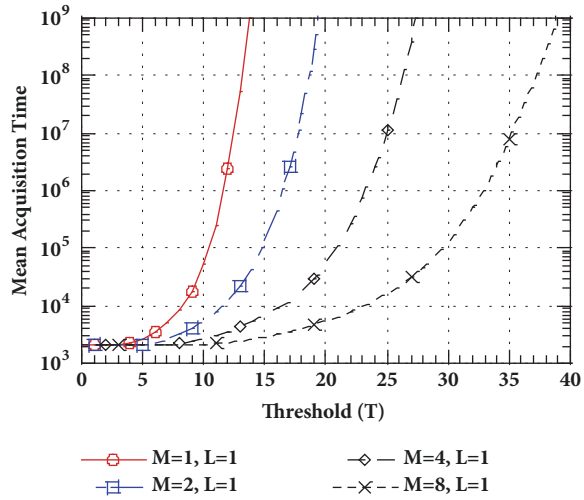

FIGURE 10: Mean acquisition time versus threshold, T, performance for the serial search acquisition of the proposed system with various transmit antennas when SNR/chip=-4dB (L=1, M=1, 2, 4, 8).

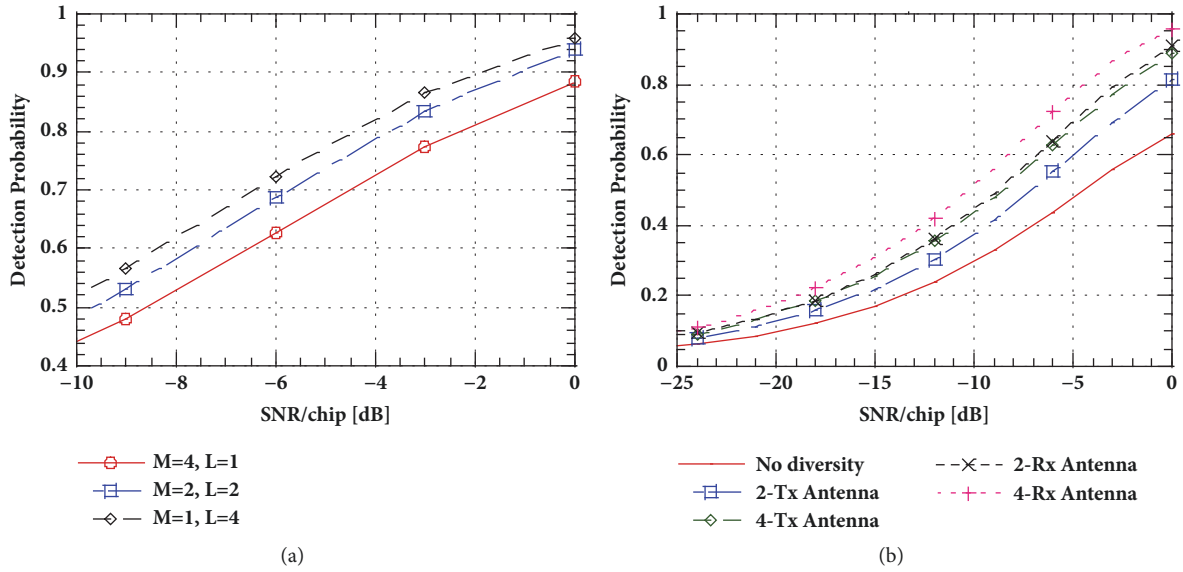

FIGURE 11: Detection probability versus SNR per chip performance of the proposed system with various transmit and receive antennas.

performance of the proposed system is significantly improved due to the diversity combining effect as the number of antennas increases.

In order to compare the acquisition performance of Tx diversity with that of Rx diversity, the detection probability, miss detection probability, and mean acquisition time of the proposed system are represented in Figures 11, 12, and 13, respectively.

Figure 11 shows the detection probabilities of the proposed system with various number of transmit and receive antennas. In Figure 11(a), the detection probability is measured for the fixed number of total antennas. The number of antennas is set to be 4. In Figure 11(b), the detection probability is tested for Tx or Rx diversity. From these results, it is confirmed that Rx diversity can enhance the detection probability much more than Tx diversity does.

In Figure 12, the miss detection probabilities are presented for several number of transmit and receive antennas. The system performance is tested in the conditions set at Figure 11. From these results, it is also shown that the miss detection probability decreases much more by using Rx diversity than by using Tx diversity.

In Figure 13, the mean acquisition time performance is shown for diverse number of transmit and receive antennas. Also, the simulation conditions are established in the same manner of the preceding conditions in Figure 11 or Figure 12. We can also see that we can improve the mean acquisition time performance much more when we employ Rx diversity than Tx diversity.

From these figures, it can be shown that Rx diversity improves the system performance much higher than Tx diversity does. This is because when Rx diversity is in use,

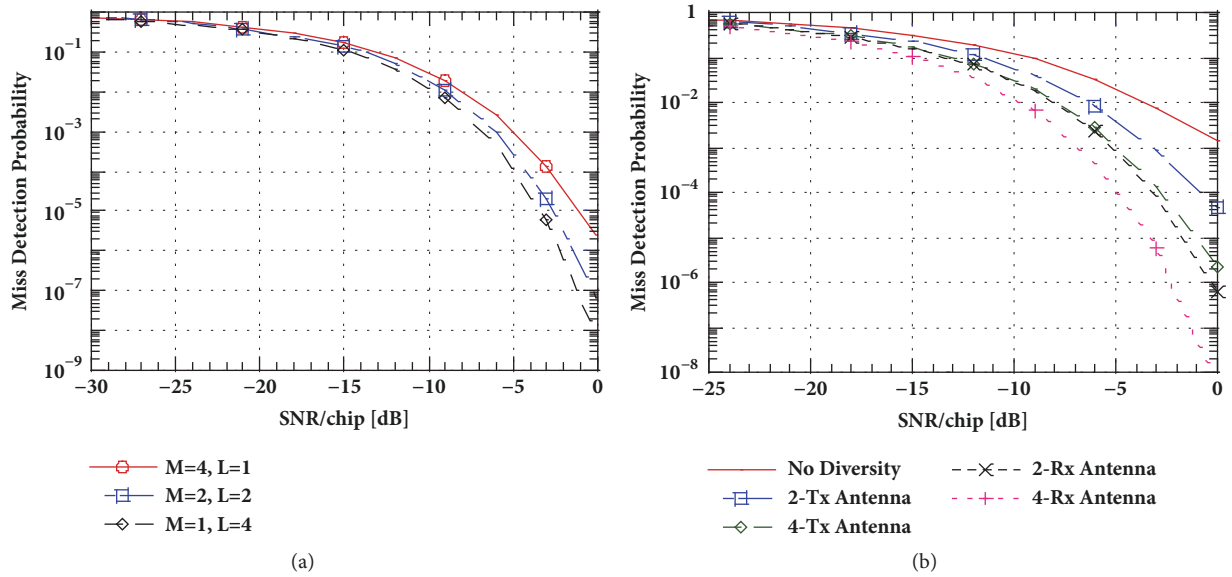

Figure 12: Miss detection probability versus SNR per chip performance of the proposed system with various transmit and receive antennas.

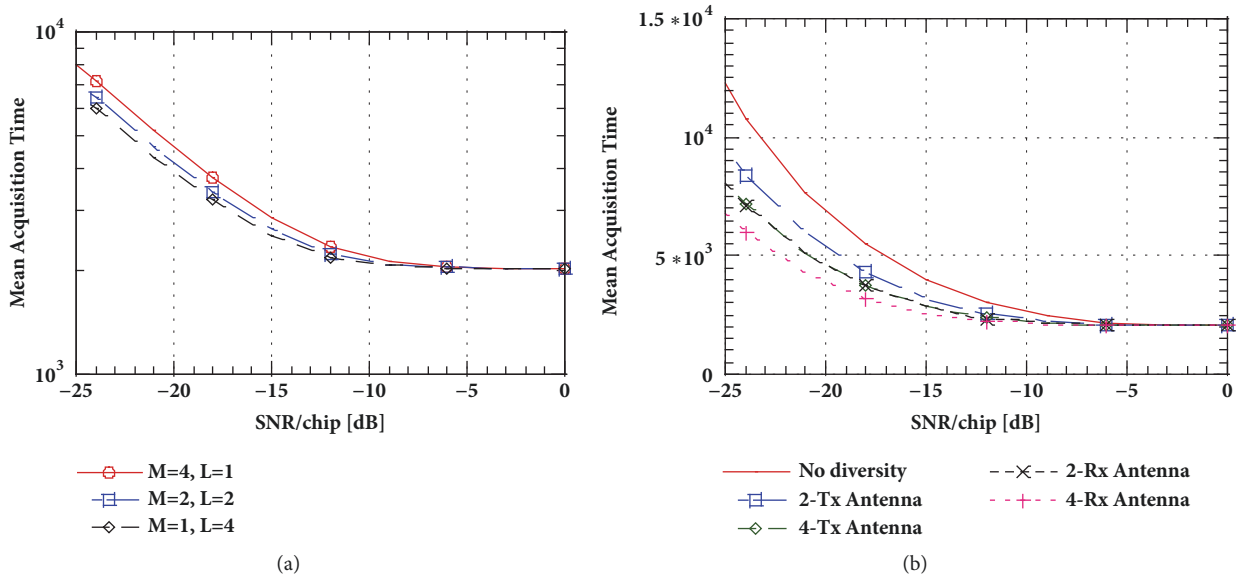

Figure 13: Mean acquisition time versus SNR/chip per chip performance for the serial search acquisition of the proposed system with various transmit and receive antennas.

we can mitigate fading to some extent and the performance improvement by using Tx diversity cannot affect much influence.

6. Conclusions and Discussions

In this paper, we have proposed Tx and Rx diversity techniques for the PN code acquisition of the UWB TH/CDMA signal in the frequency selective lognormal fading channel. In the acquisition process, we consider the hypothesis of multiple synchronous states (H_1-cells) in the uncertainty region of the PN sequence. A transmitter of the proposed system transmits the same UWB signal from different antennas at the same time but with different time delays. And a receiver of the proposed system obtains all signals from each transmitter antenna. The acquisition performance of the proposed system is evaluated when the correlator outputs of the receiver antenna associated with the same phase of the local PN code replica are noncoherently combined using EGC scheme. The closed form of the detection probability, false alarm probability, miss detection probability, and mean acquisition time are derived for the proposed system.

From the simulation results, we have shown that Tx diversity is not as effective as Rx diversity in the sense of the detection probability, the miss detection probability, and the

mean acquisition time. But the acquisition performance can be improved with Tx diversity technique. Further improvement is possible with the combination of Tx and Rx diversities if the complexity of the receiver is allowed. We have also studied the effect of the threshold on the PN code acquisition performance of the UWB system. From the results, we conclude that if the detection threshold is inappropriately set, the code acquisition performance might be significantly degraded as the number of antennas decreases. It is found that the code acquisition performance of the proposed system using the diversity combining technique becomes more robust to the detection threshold according as the number of the transmit and receive antennas increases. The proposed system can find its applications in design and implementation of various mobile and satellite communication systems.

Data Availability

The datasets generated and/or analysed during the current study are available from the corresponding author on reasonable request.

Conflicts of Interest

The authors declare that there are no conflicts of interest regarding the publication of this paper.

Acknowledgments

This work was supported in part by the Ministry of Science and ICT (MSIT), Korea, under the Information Technology Research Center (ITRC) support program (2018-0-01424) supervised by the Institute for Information & communications Technology Promotion (IITP), and in part by the Basic Science Research Program through the National Research Foundation of Korea (NRF) funded by the Ministry of Education under Grant no. NRF-2016R1D1A1B03933872.

References

[1] V. Niemelä, J. Haapola, M. Hämäläinen, and J. Iinatti, "An Ultra Wideband Survey: Global Regulations and Impulse Radio Research Based on Standards," *IEEE Communications Surveys & Tutorials*, vol. 19, no. 2, pp. 874–890, 2017.

[2] J. Y. Kim, "Ultra-wideband Wireless Communications, Seoul, Korea: GS-Intervision, 2009".

[3] J. Y. Kim and J. H. Lee, "Acquisition performance of a DS/CDMA system in a mobile satellite environment," *IEICE Trans. Commun*, vol. B, no. 1, pp. 40–48, 1997.

[4] G. Karagiannidis, S. Bouzouki, E. Karavatselou, S. Kotsopoulos, and D. Lymberopoulos, "Pseudonoise code tracking loop for a CDMA system with imperfect power control," *International Journal of Communication Systems*, vol. 14, no. 4, pp. 419–430, 2001.

[5] E. C. Kim and J. Y. Kim, "Performance Evaluation of PN Code Acquisition with Delay Diversity Receiver for TH-UWB System," in *Computational Science and Its Applications – ICCSA 2009*, vol. 5593 of *Lecture Notes in Computer Science*, pp. 226–236, Springer, Berlin, Germany, 2009.

[6] W. H. Ryu, M. K. Park, and S. K. Oh, "Code acquisition schemes using antenna arrays for DS-SS systems and their performance in spatially correlated fading channels," *IEEE Transactions on Communications*, vol. 50, no. 8, pp. 1337–1347, 2002.

[7] R. R. Rick and L. B. Milstein, "Parallel acquisition of spread-spectrum signals with antenna diversity," *IEEE Transactions on Communications*, vol. 45, no. 8, pp. 903–905, 1997.

[8] R. Tanbourgi, H. S. Dhillon, and F. K. Jondral, "Analysis of Joint Transmit-Receive Diversity in Downlink MIMO Heterogeneous Cellular Networks," *IEEE Transactions on Wireless Communications*, vol. 14, no. 12, pp. 6695–6709, 2015.

[9] S. Sangodoyin, S. Niranjayan, and A. F. Molisch, "A measurement-based model for outdoor near-ground ultrawideband channels," *Institute of Electrical and Electronics Engineers. Transactions on Antennas and Propagation*, vol. 64, no. 2, pp. 740–751, 2016.

[10] H. Hashemi, "Impulse response modeling of indoor radio propagation channels," *IEEE Journal on Selected Areas in Communications*, vol. 11, no. 7, pp. 967–978, 1993.

[11] J. Foerster, "The effects of multipath interference on the performance of UWB systems in an indoor wireless channel," in *Proceedings of the IEEE VTS 53rd Vehicular Technology Conference. Proceedings*, pp. 1176–1180, Rhodes, Greece.

[12] R. V. Hogg and E. A. Tanis, *Probability and statistical inference*, Macmillan Publishing Co., NY, USA, 1977.

[13] A. Maali, A. Mesloub, M. Djeddou, H. Mimoun, G. Baudoin, and A. Ouldali, "Adaptive CA-CFAR threshold for non-coherent IR-UWB energy detector receivers," *IEEE Communications Letters*, vol. 13, no. 12, pp. 959–961, 2009.

[14] L. G. Alberto, *Probability and Random Processes for Electrical Engineering*, Addison Wesley, 2th edition, 1994.

[15] A. Papoulis and S. Pillai, *Probability, Random Variables, and Stochastic Processes*, McGraw-Hill, NY, USA, 4th edition, 2002.

[16] R. D. Yates and D. J. Goodman, *Probability and Stochastic Processes a Friendly Introduction for Electrical and Computer Engineers*, John Wiley & Sons Ltd, 2th edition, 2005.

[17] N. C. Beaulieu, P. J. McLane, and A. A. Abu-Dayya, "Estimating the Distribution of a Sum of Independent Lognormal Random Variables," *IEEE Transactions on Communications*, vol. 43, no. 12, pp. 2869–2873, 1995.

[18] M. Abramowitz and I. A. Stegun, *Handbook of Mathematical Functions with Formulas, Graphs, and Mathematical Tables*, 9th edition, 1970.

[19] A. Polydoros and C. L. Weber, "A Unified Approach to Serial Search Spread-Spectrum Code Acquisition—Part I: General Theory," *IEEE Transactions on Communications*, vol. 32, no. 5, pp. 542–549, 1984.

[20] L.-L. Yang and L. Hanzo, "Serial acquisition of DS-CDMA signals in multipath fading mobile channels," *IEEE Transactions on Vehicular Technology*, vol. 50, no. 2, pp. 617–628, 2001.

[21] M. Z. Win and R. A. Scholtz, "Ultra-wide bandwidth time-hopping spread-spectrum impulse radio for wireless multiple-access communications," *IEEE Transactions on Communications*, vol. 48, no. 4, pp. 679–689, 2000.

[22] W. Suwansantisuk and M. Z. Win, "Multipath aided rapid acquisition: optimal search strategies," *Institute of Electrical and Electronics Engineers Transactions on Information Theory*, vol. 53, no. 1, pp. 174–193, 2007.